C Journal of Carbon Research

MDPI

Article

Char from Spent Tire Rubber: A Potential Adsorbent of Remazol Yellow Dye

Miguel Nogueira [1], Inês Matos [1], Maria Bernardo [1,*], Filomena Pinto [2], Nuno Lapa [3], Elena Surra [3] and Isabel Fonseca [1]

1 LAQV/REQUIMTE, Departamento de Química (DQ), Faculdade de Ciências e Tecnologia (FCT), Universidade Nova de Lisboa (UNL), 2829-516 Caparica, Portugal; mf.nogueira@campus.fct.unl.pt (M.N.); ines.matos@fct.unl.pt (I.M.); blo@fct.unl.pt (I.F.)

2 Unidade de Bioenergia (UB), Laboratório Nacional de Energia e Geologia (LNEG), Estrada do Paço do Lumiar, Ed. J, 1649-038 Lisboa, Portugal; filomena.pinto@lneg.pt

3 LAQV/REQUIMTE, Departamento de Ciências e Tecnologia da Biomassa (DCTB), Faculdade de Ciências e Tecnologia (FCT), Universidade Nova de Lisboa (UNL), 2829-516 Caparica, Portugal; ncsn@fct.unl.pt (N.L.); e.surra@campus.fct.unl.pt (E.S.)

* Correspondence: maria.b@fct.unl.pt; Tel.: +351-212948300

Received: 10 October 2019; Accepted: 14 November 2019; Published: 18 November 2019

Abstract: A char produced from spent tire rubber showed very promising results as an adsorbent of Remazol Yellow (RY) from aqueous solutions. Spent tire rubber was submitted to a pyrolysis process optimized for char production. The obtained char was submitted to chemical, physical, and textural characterizations and, subsequently, applied as a low-cost adsorbent for dye (RY) removal in batch adsorption assays. The obtained char was characterized by relatively high ash content (12.9% wt), high fixed-carbon content (69.7% wt), a surface area of 69 m^2/g, and total pore volume of 0.14 cm^3/g. Remazol Yellow kinetic assays and modelling of the experimental data using the pseudo-first and pseudo-second order kinetic models demonstrated a better adjustment to the pseudo-first order model with a calculated uptake capacity of 14.2 mg RY/g char. From the equilibrium assays, the adsorption isotherm was fitted to both Langmuir and Freundlich models; it was found a better fit for the Langmuir model to the experimental data, indicating a monolayer adsorption process with a monolayer uptake capacity of 11.9 mg RY/g char. Under the experimental conditions of the adsorption assays, the char presented positive charges at its surface, able to attract the deprotonated sulfonate groups (SO_3^-) of RY; therefore, electrostatic attraction was considered the most plausible mechanism for dye removal.

Keywords: tire rubber; char; dye; adsorption

1. Introduction

The development of advanced societies and industries is associated with the generation of elevated quantities of wastes and the release of contaminants into nature. Spent tires (STs) and dyes represent two of these pollutants and are an ever-growing environmental threat. In order to provide efficient solutions for waste valorization and wastewater decontamination, pathways that provide solutions to these contaminants while fomenting the concept of circular economy must be strengthened.

The disposal of STs represents a major environmental threat worldwide. In 2017, Valorpneu (Portuguese Management Company of the Integrated System for Used Tires) reported that approximately 80,000 tons of tires were disposed of in Portugal [1], while, in Europe, this value reached almost 4 million tons [2]. High percentages of these wastes (25% in Portugal) are sent for energy valorization in cement kilns [1] which implies material loss as well as the possible emission of greenhouse gases and toxic compounds. In this context, ST recycling must be strengthened with new

solutions based on the concept of material valorization. Pyrolysis (also known as chemical recycling) has demonstrated to be a viable route for ST valorization, as it effectively converts wastes into high added-value products, such as chars and other materials, that can be used in different industries in a wide range of applications [3–5]. Among the possible applications for ST-derived chars, their singular properties turn them into potential adsorbents for the removal of pollutants from contaminated wastewaters [5–8].

Organic dyes are generally used in textile, plastic, food, and paper industries. Their effluents are some of the main sources of water contamination. Often, the effluents are discarded into water bodies even if they are contaminated with anionic dyes, such as Remazol Yellow (RY). This dye belongs to the class of azo dyes [9,10] which is a group of compounds with a rising cause of concern due to the fact of its toxic, carcinogenic, and mutagenic properties that can threaten human life and aquatic ecosystems [11,12]. Wastewater treatment before its discharge into environmental compartments is imperative to ensure environmental safety and diminish the human health impacts associated to these dyes. Adsorption has shown to be one of the most efficient options due to the fact of its potentially low economic and environmental impacts and high capacity for up-scaling to industrial levels [13–15].

Spent tire-derived chars have been applied as removal agents for many different dyes from wastewaters, such as Methylene Blue [7,8], Congo Red [16], Acid Yellow 117 (AY117), and Acid Blue 25 (AB25) [17], among others. However, the use of these types of chars as adsorbents of RY dye has not yet been reported. In this context, the main aims of this work were (i) the production and characterization of a char obtained from the pyrolysis of spent tire rubber and (ii) its ulterior application as an adsorbent for the removal of RY dye from synthetic wastewater. Remazol Yellow was used in this work as a model azo dye molecule. The obtained char was submitted to several chemical and textural characterizations in order to investigate their surface and inner properties. The uptake rate and uptake capacity of the dye molecules were determined thought kinetic and equilibrium adsorption assays.

2. Materials and Methods

2.1. Spent Tire Rubber

Spent tire rubber was collected in a Portuguese mechanical recycling facility and used as the feedstock material for the pyrolysis assays. It was ground and sieved to a 2–4 mm particle size. This sample was subsequently submitted to the following characterizations:

(i) Proximate analysis through a gravimetric method in order to determine the moisture content (105 °C), volatile matter (950 °C), and ashes (750 °C);
(ii) Elemental analysis to quantify C, H, N, and S (Thermo Finnigan-CE Instruments Flash EA 1112 CHNS analyzer, Waltham, USA);
(iii) Thermogravimetric analysis (TGA) between room temperature and 900 °C, with a heating rate of 5 °C/min, under an argon atmosphere (Setaram Labsys EVO equipment, France).

2.2. Pyrolysis Assays and Chars

The pyrolysis assays were carried out in a 5.5 dm^3 stirred batch reactor (Parr Instruments, Hastelloy C276, Illinois, USA) which was purged and pressurized to 0.6 MPa with nitrogen (N_2). A heating rate of 5 °C/min was applied until the desired reaction temperature of 405 °C had been reached, which was then held for 30 min. After cooling to room temperature, the char was separated from the liquid fraction by settling and extraction with hexane. The char obtained was coded as CPN and submitted to the following characterizations:

(i) Proximate analysis, elemental analysis, and TGA as described above;
(ii) Mineral content, performed according to the European Standard EN 15290 in samples previously digested (3 cm^3 H_2O_2 30% *v*/*v* + 8 cm^3 HNO_3 65% *v*/*v* + 2 cm^3 HF 40% *v*/*v*) in a microwave

station (Milestone Ethos 1600 Microwave Labstation, Italy) and neutralized (20 cm^3 H_3BO_3 4% *w*/*v*). The acidic solutions were analyzed by inductively coupled plasma–atomic emission spectroscopy (ICP-AES) (Horiba Jobin-Yvon equipment, France) for the quantification of several chemical elements;

(iii) pH_{PZC}, for which 20 mL of NaCl 0.1 M were transferred to polyethylene bottles for pH adjustment with HCl 0.1 M or NaOH 0.1 M. The assay was performed with different initial pH values: 2, 4, 6, 8, 10, and 12. After pH adjustment, 0.1 g of char was added to each bottle. These mixtures were then agitated for 24 h in a roller-table device. After mixing, all samples were filtrated, and the final pH was then measured. The pH_{PZC} value corresponds to the plateau of the curve pH_{final} versus $pH_{initial}$;

(iv) X-ray powder diffraction (XRPD), in which the diffractogram was obtained using a benchtop X-ray diffractometer (RIGAKU, model MiniFlex II, USA), with a Cu X-ray tube (30 kV/15 mA) by continuous scanning from 15° to 80° (2θ) with a step size of 0.01° (2θ) and scan speed of 2°/min;

(v) Scanning electron microscopy with energy-dispersive X-ray spectrometry (SEM-EDS), for which the surface elemental composition and morphology of the char were analyzed using a JEOL 7001F analytical FEG-SEM with Oxford model INCA 250 PREMIUM EBSD (electron backscatter diffraction) and energy-dispersive X-ray spectrometer light element detector attachments (Japan);

(vi) N_2 adsorption–desorption isotherms at 77 K, for which the isotherms were obtained in a ASAP 2010 Micromeritics equipment (USA) and allowed to calculate the following parameters: (1) apparent surface area using the BET (Brunauer–Emmett–Teller) equation (A_{BET}); (2) total pore volume determined by the amount of nitrogen adsorbed at $P/P_0 = 0.95$ (V_{total}); (3) micropore volume using the t-plot method (V_{micro}); and (4) mesopore volume by the difference between V_{total} and V_{micro}. Prior to this analysis, the samples were outgassed overnight, under vacuum, at 150 °C.

2.3. Adsorption Assays

The dye chosen for the adsorption studies was Remazol Yellow 3RS 133% (Dystar, Singapore), CAS number: 140876-15-9. This is an anionic sulfonated azo dye and its molecular structure is presented in Figure 1. Stock solutions containing 200 mg/dm^3 of RY were prepared everyday using deionized water and posteriorly diluted to obtain different working concentrations. Batch adsorption experiments were performed in 10 mL vials, at 25 ± 1 °C, under constant agitation (1000 rpm) and dark environment. To investigate the effects of pH (2–6) and adsorbent dosage (1–4 g/dm^3), an initial concentration of 20 mg/dm^3 of RY and a contact time of 150 min were used. The study on the effect of contact time (kinetic study) was performed up to 360 min, at the natural pH of RY solution (6.0), an initial concentration of 100 mg/dm^3, and an adsorbent dosage of 4 g/dm^3. The influence of different initial concentrations (equilibrium studies) was performed at an adsorbent dosage of 4 g/dm^3, contact time of 150 min, and an initial dye concentration in the interval of 20–200 mg/dm^3.

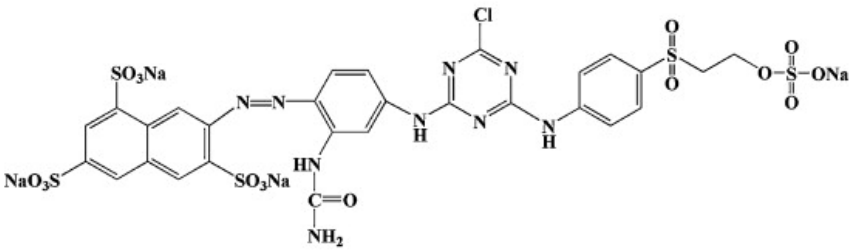

Figure 1. Chemical structure of Remazol Yellow 3RS.

After the adsorption assays, the samples were filtrated with Mixed Cellulose Ester (MCE) membranes of 0.22 μm pore size. Dye concentration in the filtrated solution was measured from calibration curves using UV-Vis at 414 nm in a GBC 916 spectrophotometer. The dye removal efficiency

(R in %) and amount of dye adsorbed per unit mass (q_{exp} in mg/g) were calculated using Equations (1) and (2), respectively:

$$R = \frac{\left(C_0 - C_f\right)}{C_0} \times 100. \quad (1)$$

$$q_{exp} = \frac{\left(C_0 - C_f\right)}{m} \times V \quad (2)$$

where C_0 and C_f (mg/dm^3) are the initial and final concentrations of dye in solution, respectively, V (dm^3) is the volume of solution, and m (g) is the amount of the adsorbent used.

The kinetic data were modelled through pseudo-first and pseudo-second order kinetic models (Equations (3) and (4), respectively) to describe adsorption data obtained under non-equilibrium conditions [18–20]. These kinetic models assume that the process is controlled by the irreversible adsorption reaction at the liquid/solid interface in the adsorbent, neglecting the effects of film and pore diffusion; the uptake rate is first or second order with respect to the available surface coverage.

$$q_t = q_e \times \left(1 - e^{-k_1 \times t}\right) \quad (3)$$

$$q_t = \frac{k_2 \times q_e^2 \times t}{1 + q_e \times k_2 \times t} \quad (4)$$

where q_t is the uptake capacity of RY at time t (mg/g), q_e is the uptake capacity at equilibrium (mg/g), k_1 is the pseudo-first order kinetic constant (1/min), k_2 is the pseudo-second order kinetic constant (g/(mg.min)), and t is the contact time (min).

The experimental data from the equilibrium studies were modelled by Langmuir (Equation (5)) and Freundlich (Equation (6)) models [21,22]:

$$q_e = \frac{q_{max} \times K_L \times C_e}{1 + K_L \times C_e} \quad (5)$$

$$q_e = K_F \times C_e^{\frac{1}{n}} \quad (6)$$

where q_e is the adsorbent removal capacity in the equilibrium (mg/g), q_{max} is the maximum uptake capacity or the monolayer capacity (mg/g), K_L is the Langmuir's constant (L/mg), C_e is the concentration of RY in the equilibrium (mg/L), K_F is the Freundlich's constant (mg$^{(1-1/n)}$ L$^{1/n}$/g) and $\frac{1}{n}$ is the adsorption intensity (dimensionless). The Langmuir model assumes that the active sites on the surface are energetically homogeneous; once a sorbate molecule occupies a site, no further adsorption can take place at that site [23]. Thus, there is no interaction among molecules adsorbed on adjacent or near sites, and the phenomenon runs until the complete formation of the monolayer; adsorption is localized, and the energy needed for the process does not depend on the coverage degree. The Freundlich model conceives an energetic heterogeneity of the active sites, considering multilayer formation [23].

The modelling of experimental data from kinetic and equilibrium assays was performed with the Solver add-in of MS Excel by using the minimization criterion of the sum of least squares.

3. Results and Discussion

3.1. ST Rubber and Char Characterization

The char yield in the pyrolysis assays was 37.9% wt after hexane extraction. Proximate analysis (Table 1) showed that the feedstock (ST rubber) and char had fixed-carbon percentages of 27.8% and 69.7% wt, respectively, indicating that the pyrolysis process was successful in converting the spent rubber into char. The ash content was high in the char (12.9% wt), resulting from the concentration effect of pyrolysis. Elemental analysis (Table 1) demonstrated that the char had high carbon and sulfur contents, 86.7% and 2.67% wt, respectively. The sulfur was used in the vulcanization process of tire

rubber [24]. The char composition is in line with already reported tire-derived chars [25–27]. The char presented a pH_{PZC} value of 6.80, indicating a neutral surface [8].

Table 1. Proximate [a] and elemental [a] analyses, and pH_{PZC} for both ST rubber and char (% wt).

Parameter	Moisture	Volatile Matter	Fixed Carbon [b]	Ashes	C	H	N	S	pH_{PZC}
ST rubber	0.43	68.9	27.7	2.96	86.8	7.36	0.00	1.23	n.d.
Char	0.70	16.7	69.7	12.9	86.7	0.83	0.00	2.67	6.80

[a] As-received basis; [b] fixed carbon = 100 − (moisture + volatile matter + ashes); n.d. = not determined.

Thermogravimetric curves are presented in Figure 2 for both ST rubber and char. A mass loss of 70% of ST rubber occurred up to around 440 °C from which the thermal degradation stabilized, remaining around 30% of carbonaceous residue. The char still lost around 18% (a fraction of this loss is related to water release) of its mass up to 900 °C, indicating the presence of some unconverted carbon [28,29].

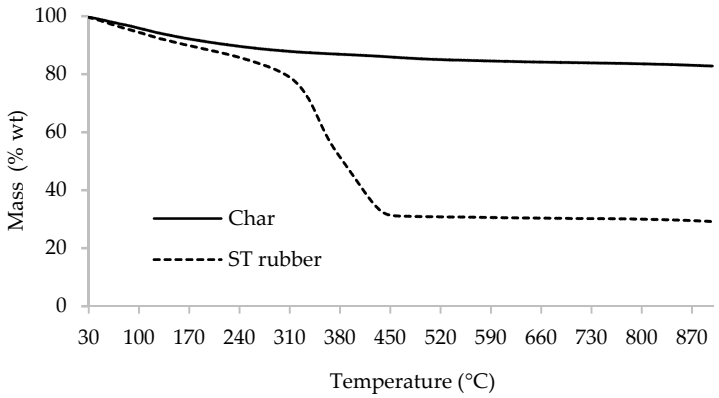

Figure 2. The TGA curves for both spent tire (ST) rubber and char samples.

The mineral analysis of char (Table 2) revealed the presence of many metals and metalloids, but the high concentrations of zinc and silicon stood out. In fact, zinc oxide (ZnO) and silica (SiO_2) are used in tire manufacturing [24,30].

Table 2. Mineral content (mg/kg db) of ST char.

Element	mg/kg db (X ± σ)
Zn	37,543 ± 5251
Si	11,212 ± 1011
Al	2800 ± 335
Na	2534 ± 765
Ba	1882 ± 195
K	1796 ± 477
Ca	1588 ± 495
Mg	576 ± 55.5
P	501 ± 53.2
Ni	123 ± 28.6
Ti	110 ± 16
Pb	42.4 ± 5.33
Sb	10.1 ± 1.45
Mo	7.33 ± 1.24
As	5.99 ± 1.46
Cd	3.53 ± 0.441

db—dry basis; standard deviations (σ) of duplicates are presented.

The XRPD analysis allowed identifying the main crystalline mineral phases in char composition. The XRD pattern (Figure 3) is typical of ST-derived chars, as the peaks observed were mainly attributed to zinc sulfide (ZnS) [25,31,32]. The ZnO used as accelerator in rubber vulcanization suffers sulfidation with the hydrogen sulfide (H_2S) generated during ST rubber pyrolysis [33,34].

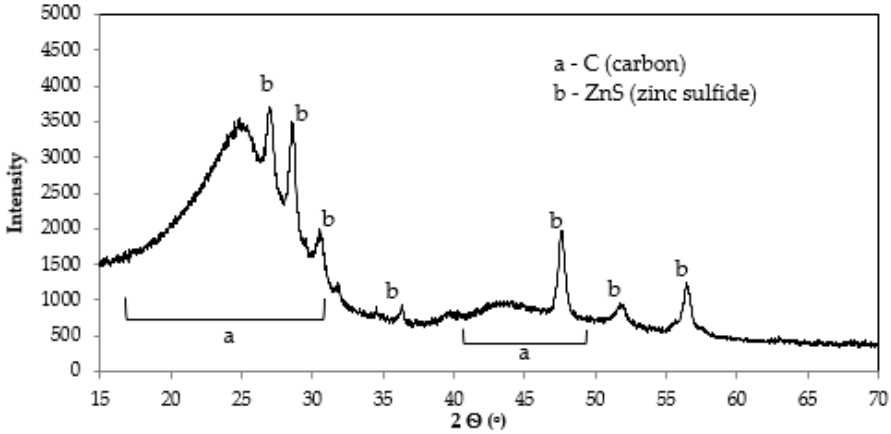

Figure 3. The XRD pattern of ST char.

The broad peaks between 15° and 30° and 40° and 50° (2θ) corresponded to an amorphous carbon structure with randomly arranged graphite-like microcrystalite structures [32,35].

The N_2 adsorption–desorption isotherm, at 77 K, and the textural parameters obtained from the isotherm for char are shown in Figure 4 and Table 3, respectively.

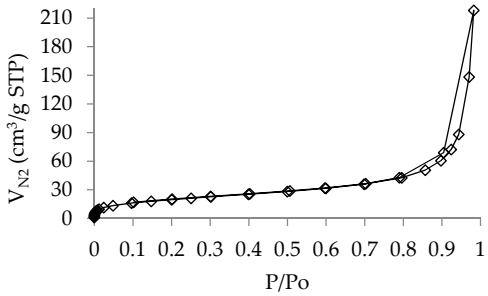

Summary Data	
A_{BET} (m^2/g)	69
V_{micro} (cm^3/g)	0.01
V_{meso} (cm^3/g)	0.13
V_{total} (cm^3/g)	0.14

Figure 4. N_2 adsorption–desorption isotherm at 77 K of the char sample and textural parameters calculated from the isotherm.

Table 3. Parameters obtained from kinetic modelling and from Langmuir and Freundlich modelling for RY adsorption on ST-derived char.

Pseudo-First Order Kinetic Model			Pseudo-Second Order Kinetic Model		
R^2	q_e, calc (mg/g)	k_1 (1/min)	R^2	q_e, calc (mg/g)	k_2 (g/(mg.min))
0.952	14.2	0.008	0.942	19.8	0.0003
Langmuir			**Freundlich**		
R^2	q_{max} (mg/g)	K_L (L/mg)	R^2	K_F (mg $^{(1-1/n)}$ $L^{1/n}$/g)	1/n
0.998	11.9	0.514	0.945	5.43	0.174

R^2—determination coefficient; q_e—adsorbate uptake at equilibrium; calc—calculated; k_2—pseudo-second order kinetic constant; k_1—pseudo-first order kinetic constant; q_{max}—maximum uptake capacity or monolayer capacity; K_L—Langmuir's constant; K_F—Freundlich's constant; $\frac{1}{n}$—adsorption intensity.

The char presented an isotherm of type II according to the IUPAC classification [36], which is typical of non-porous or macroporous materials, representing unrestricted monolayer–multilayer adsorption.

However, the presence of the hysteresis loop indicates some mesoporosity [37]. This hysteresis loops is of Type H3, usually given by non-rigid aggregates of plate-like particles, but also for the case in which the pore network consists of macropores not completely filled up with pore condensate [36]. The char presented an apparent surface area (A_{BET}) of 69 m^2/g and total pore volume (V_{total}) of 0.14 cm^3/g, most of which corresponded to mesopores. This isotherm profile is typical of tire-derived chars, being largely determined by the carbon black from the original tire material that remains in the chars after pyrolysis [27,32,35].

The SEM image of the char particles (Figure 5) shows a rough surface with nanosized mineral clusters. This rough and heterogeneous morphology at the char surface has already been observed in tire-derived char particles [25,32,35]. The EDS spectra indicated that the char particles were carbonaceous in nature and the agglomerated mineral clusters were composed mainly of ZnS which is in accordance with the XRPD analysis.

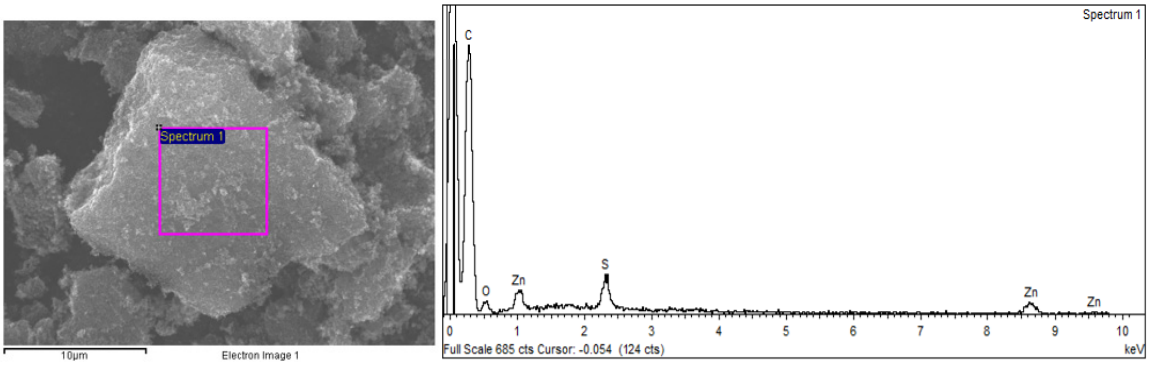

Figure 5. SEM images of char particles with a magnification of 4000× (**left**) and EDS spectra (**right**).

3.2. Adsorption Assays

To evaluate the effect of pH in the adsorption process, RY removal assays were performed at pH 2.0, 4.0, and 6.0, the latter corresponding to the natural pH of the dye solution. The range of pH chosen was based on the fact that the pH_{PZC} value of the char was 6.8, being expected that above this value the char surface becomes negatively charged, repelling the deprotonated sulfonate groups (SO_3^-) [38]. The obtained results (results not shown) surprisingly demonstrated that the pH had no significant effect on the adsorption process. It was expected that at the low pH 2, the dye molecule becomes increasingly protonated, leading to a decrease on its removal by an electrostatic interaction mechanism. The fact that no differences were observed on the removal percentages indicates that other removal mechanisms played an important role at the low pH value. Given the results obtained, the following assays were performed without pH adjustment.

The study on adsorbent dosage (Figure 6) indicated that a S/L ratio of 4 g/dm^3 gave the highest average removal percentages of RY (almost 100%). This was expected, as the higher the mass of adsorbent used, the higher the removal of RY because more adsorption sites are available. However, the difference between the adsorbent dosages of 2 and 4 g/dm^3 was small. High adsorbent dosages of chars usually do not provide benefits on the adsorption process, since it is observed as an agglomeration effect of the char particles, reducing the surface area available for adsorption [39,40].

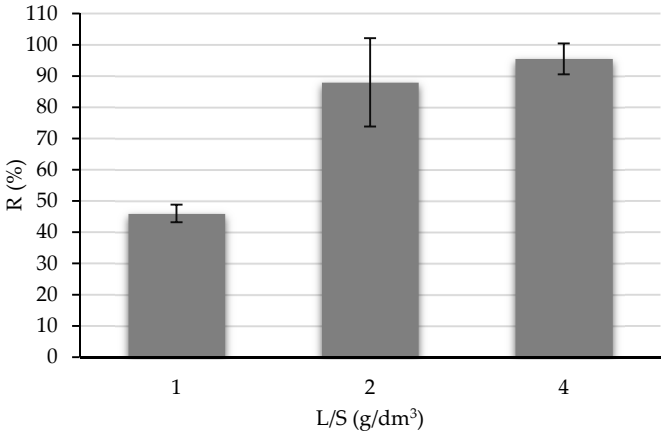

Figure 6. Effect of char dosage on the removal of Remazol Yellow (RY) from solution. Conditions: initial RY concentration = 20 mg/dm^3; solution pH = natural; contact time = 150 min. Error bars of duplicates are presented.

Figure 7 presents the experimental kinetic data on RY removal by ST-derived char. It seems that equilibrium was attained at approximately 150 min with an uptake capacity of approximately 12 mg RY/g char, since a significant increase in the experimental uptake capacity of RY above this contact time was not observed. At equilibrium, the char removed around 43% RY.

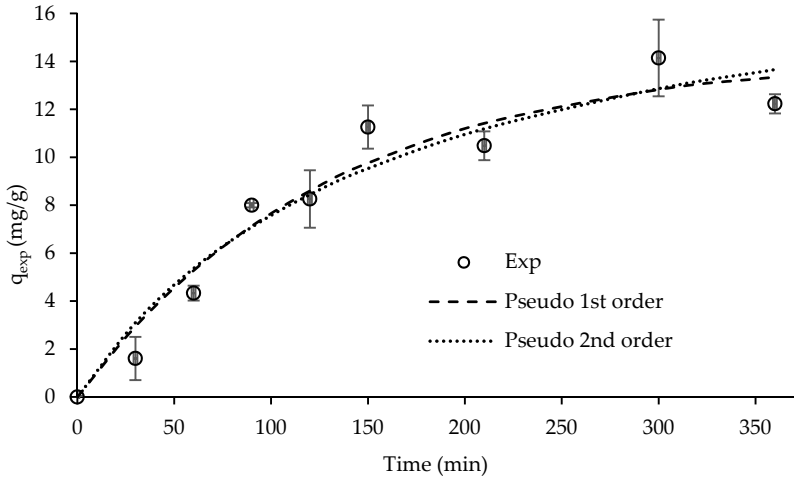

Figure 7. Kinetic data of RY removal by ST-derived char adjusted to pseudo-first and pseudo-second order kinetic models. Conditions: RY initial concentration = 100 mg/dm^3; solution pH = 6.0 (natural); char dosage = 4 g/dm^3. Exp—experimental data. Error bars of duplicates are shown.

Table 3 presents the kinetic parameters obtained from the fitting of both pseudo-first order and pseudo-second order kinetic models to the experimental kinetic data. The pseudo-first order kinetic model presented a slightly better adjustment with a calculated uptake capacity of 14.2 mg RY/g char.

Based on the kinetic study, an equilibrium time of 150 min was chosen for adsorption isotherm assays (effect of initial RY concentration).

Figure 8 shows the adsorption isotherm data of RY and the adjustments for Langmuir and Freundlich models. The obtained parameters from the models are presented in Table 3.

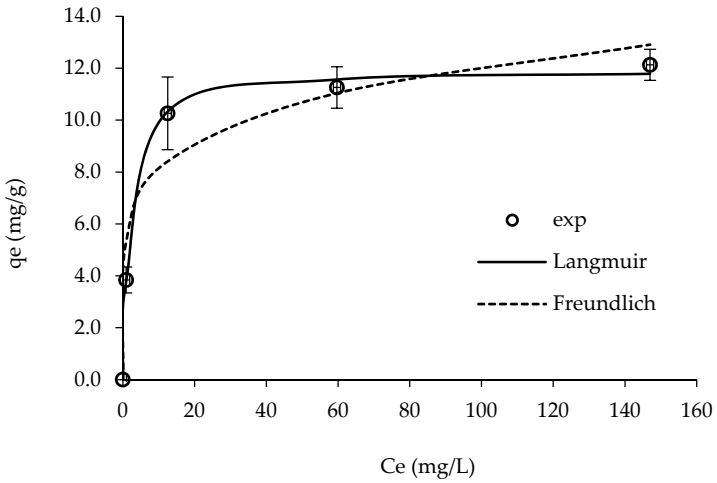

Figure 8. Experimental data and fits of the Langmuir and Freundlich models for the adsorption of RY on ST-derived char. Conditions: contact time = 150 min; solution pH = 6.0 (natural); char dosage = 4 g/dm^3. Exp—experimental data. Error bars of duplicates are shown.

The results showed that the experimental data were better adjusted to the Langmuir model, suggesting that the adsorption occurred through a monolayer process [23]. The maximum RY uptake capacity was 11.9 mg/g, which is comparable or even slightly higher to the performance of other adsorbent materials, such as zeolites and biomass fly ashes as reported in literature (Table 4). Nevertheless, other types of zeolites and chitosan presented a much higher uptake capacities of RY dye (Table 4).

Table 4. RY uptake capacities of different adsorbent materials found in the literature.

Adsorbent	q_{max} (mg/g)	Reference
ST rubber-derived char	11.9	Present work
Natural and modified zeolites	5.54–13.2	[41]
Zeolite and sepiolite	88.5–169	[42]
Chitosan	311–928	[38]
Biomass fly ash	3.65	[43]

As already mentioned, electrostatic interaction between the positively charged char surface and the deprotonated sulfonate groups (SO_3^-) is a plausible mechanism for RY removal by this char [38,43]. However, other possible mechanisms, such as π–π bonding between the aromatic rings of the carbonaceous matrix of the char and the aromatic rings of the organic molecule (Figure 1), cation–π interactions between the cations of the char (Table 2), and the aromatic rings of dye molecule, the complexation of char cations with the anionic dye, or even pore filling mechanism (the meso and macropores of the inner matrix of the char are able to accommodate the large molecules of RY dye) should not be discarded [17,40,44–46]. Still, it is difficult to account for the contribution of each mechanism.

4. Conclusions

The obtained char demonstrated the potential to be used as a low-cost adsorbent for Remazol Yellow dye from aqueous solutions.

The produced char showed a 12.9% ash content, a surface area of 69 m^2/g, high percentages of fixed carbon, and a neutral surface. In the RY removal assays, the char showed to be efficient with almost 100% removal efficiency at the natural RY pH (6.0), adsorbent dosage of 4 g/dm^3, and initial dye concentration of 20 mg/dm^3. Kinetic assays and modelling of the experimental data demonstrated a better adjustment to the pseudo-first order kinetic model with a calculated uptake capacity of 14.2 mg

RY/g char. From the equilibrium assays (adsorption isotherm), the experimental data was found to better fit the Langmuir model, indicating a monolayer adsorption process with a monolayer uptake capacity of 11.9 mg RY/g char. Electrostatic interaction between the positively charged char surface and the deprotonated sulfonate groups (SO_3^-) of RY was considered to be the most plausible mechanism for dye removal.

Pyrolysis showed to be a viable route for the valorization of spent tire rubber. The process produced chars with suitable properties for application as low-cost adsorbents for wastewater decontamination, besides being viable precursors for further valorization into activated carbons.

Author Contributions: Conceptualization, I.M. and N.L.; Formal analysis, M.N., M.B. and E.S.; Funding acquisition, I.M., M.B., N.L. and I.F.; Investigation, M.N., M.B., F.P. and E.S.; Methodology, I.M., M.B., F.P. and E.S.; Project administration, N.L. and I.F.; Resources, I.M., F.P., N.L. and I.F.; Supervision, I.M., N.L. and I.F.; Validation, I.M., M.B. and N.L.; Visualization, M.N.; Writing – original draft, M.B.; Writing – review & editing, M.N., I.M., F.P., N.L., E.S. and I.F.

Funding: The authors thank Valorpneu for the "Inov.Ação 2018" award. This work was also supported by the Associate Laboratory for Green Chemistry-LAQV which is financed by Portuguese funds from FCT/MCTES (UID/QUI/50006/2019). Ines Matos thanks FCT/MCTES for the "Investigador FCT" contract.

Conflicts of Interest: The authors declare no conflict of interest.

References

1. Valorpneu - Sociedade de Gestão de Pneus, LDA. *Relatorio Anual e Contas 2017*; Valorpneu - Sociedade de Gestão de Pneus, LDA: Lisboa, Portugal, 2017.
2. ETRMA - European Tyre and Rubber Manufacturers Association. *ELT Management Figures 2016*; ETRMA - European Tyre and Rubber Manufacturers Association: Brussels, Belgium, 2018.
3. Parthasarathy, P.; Choi, H.S.; Park, H.C.; Hwang, J.G.; Yoo, H.S.; Lee, B.-K.; Upadhyay, M. Influence of Process Conditions on Product Yield of Waste Tyre Pyrolysis- A Review. *Korean J. Chem. Eng.* **2016**, *33*, 2268–2286. [CrossRef]
4. Sathiskumar, C.; Karthikeyan, S. Recycling of Waste Tires and Its Energy Storage Application of By-Products – a Review. *Sustain. Mater. Technol.* **2019**, *22*, e00125. [CrossRef]
5. Saleh, T.A.; Gupta, V.K. Processing Methods, Characteristics and Adsorption Behavior of Tire Derived Carbons: A Review. *Adv. Colloid Interface Sci.* **2014**, *211*, 93–101. [CrossRef] [PubMed]
6. Antoniou, N.; Stavropoulos, G.; Zabaniotou, A. Activation of End of Life Tyres Pyrolytic Char for Enhancing Viability of Pyrolysis – Critical Review, Analysis and Recommendations for a Hybrid Dual System. *Renew. Sustain. Energy Rev.* **2014**, *39*, 1053–1073. [CrossRef]
7. Makrigianni, V.; Giannakas, A.; Hela, D.; Papadaki, M.; Konstantinou, I. Adsorption of Methylene Blue Dye by Pyrolytic Tire Char in Fixed-Bed Column. *Desalin. WATER Treat.* **2017**, *65*, 346–358. [CrossRef]
8. Makrigianni, V.; Giannakas, A.; Deligiannakis, Y.; Konstantinou, I. Adsorption of Phenol and Methylene Blue from Aqueous Solutions by Pyrolytic Tire Char: Equilibrium and Kinetic Studies. *J. Environ. Chem. Eng.* **2015**, *3*, 574–582. [CrossRef]
9. Kiernan, J. Classification and Naming of Dyes, Stains and Fluorochromes. *Biotech. Histochem.* **2001**, *76*, 261–278. [CrossRef]
10. Ajmal, A.; Majeed, I.; Malik, R.N.; Idriss, H.; Nadeem, M.A. Principles and Mechanisms of Photocatalytic Dye Degradation on TiO 2 Based Photocatalysts: A Comparative Overview. *RSC Adv.* **2014**, *4*, 37003–37026. [CrossRef]
11. Ratna, P.B. Pollution Due to Synthetic Dyes Toxicity & Carcinogenicity Studies and Remediation. *Int. J. Environ. Sci.* **2012**, *3*, 940–955. [CrossRef]
12. Rawat, D.; Mishra, V.; Sharma, R.S. Detoxification of Azo Dyes in the Context of Environmental Processes. *Chemosphere* **2016**, *155*, 591–605. [CrossRef]
13. Mondal, S.; Purkait, M.K.; De, S. *Advances in Dye Removal Technologies*; Green Chemistry and Sustainable Technology; Springer Singapore: Singapore, 2018. [CrossRef]
14. Yagub, M.T.; Sen, T.K.; Afroze, S.; Ang, H.M. Dye and Its Removal from Aqueous Solution by Adsorption: A Review. *Adv. Colloid Interface Sci.* **2014**, *209*, 172–184. [CrossRef] [PubMed]

15. Zhou, Y.; Lu, J.; Zhou, Y.; Liu, Y. Recent Advances for Dyes Removal Using Novel Adsorbents: A Review. *Environ. Pollut.* **2019**, *252*, 352–365. [CrossRef] [PubMed]
16. Aftab, T.; Bashir, F.; Khan, R.A.; Iqbal, J. Treatment of Color through the Adsorption Efficiency of Waste Tire-Derived Char Using Response Surface Methodology. *Desalin. Water Treat.* **2016**, *57*, 10324–10332. [CrossRef]
17. Chan, O.S.; Cheung, W.H.; McKay, G. Single and Multicomponent Acid Dye Adsorption Equilibrium Studies on Tyre Demineralised Activated Carbon. *Chem. Eng. J.* **2012**, *191*, 162–170. [CrossRef]
18. Lagergren, S. About the Theory of So-Called Adsorption of Soluble Substances. *K. Sven. Vetenskapsakademiens. Handl.* **1898**, *24*, 1–39.
19. Ho, Y.S.; McKay, G. Sorption of Dye from Aqueous Solution by Peat. *Chem. Eng. J.* **1998**, *70*, 115–124. [CrossRef]
20. Sharma, Y.C.; Gupta, G.S.; Prasad, G.; Rupainwar, D.C. Use of Wollastonite in the Removal of Ni(II) from Aqueous Solutions. *Water. Air. Soil Pollut.* **1990**, *49*, 69–79. [CrossRef]
21. Foo, K.Y.; Hameed, B.H. Insights into the Modeling of Adsorption Isotherm Systems. *Chem. Eng. J.* **2010**, *156*, 2–10. [CrossRef]
22. Limousin, G.; Gaudet, J.P.; Charlet, L.; Szenknect, S.; Barthès, V.; Krimissa, M. Sorption Isotherms: A Review on Physical Bases, Modeling and Measurement. *Appl. Geochem.* **2007**, 249–275. [CrossRef]
23. Russo, V.; Trifuoggi, M.; Di Serio, M.; Tesser, R. Fluid-Solid Adsorption in Batch and Continuous Processing: A Review and Insights into Modeling. *Chem. Eng. Technol.* **2017**, *40*, 799–820. [CrossRef]
24. Coran, A.Y. Vulcanization. In *The Science and Technology of Rubber*; Elsevier: Amsterdam, The Netherlands, 2013; pp. 337–381. [CrossRef]
25. Zhou, Q.; Zarei, A.; De Girolamo, A.; Yan, Y.; Zhang, L. Catalytic Performance of Scrap Tyre Char for the Upgrading of Eucalyptus Pyrolysis Derived Bio-Oil via Cracking and Deoxygenation. *J. Anal. Appl. Pyrolysis* **2019**, *139*, 167–176. [CrossRef]
26. Preciado-Hernandez, J.; Zhang, J.; Zhu, M.; Zhang, Z.; Zhang, D. An Experimental Study of CO2 Gasification Kinetics during Activation of a Spent Tyre Pyrolysis Char. *Chem. Eng. Res. Des.* **2019**, *149*, 129–137. [CrossRef]
27. Chan, O.S.; Cheung, W.H.; McKay, G. Preparation and Characterisation of Demineralised Tyre Derived Activated Carbon. *Carbon N. Y.* **2011**, *49*, 4674–4687. [CrossRef]
28. Husár, J.; Haydary, J.; Šuhaj, P.; Steltenpohl, P. Potential of Tire Pyrolysis Char as Tar-Cracking Catalyst in Solid Waste and Biomass Gasification. *Chem. Pap.* **2019**, *73*, 2091–2101. [CrossRef]
29. Han, J.; Li, W.; Liu, D.; Qin, L.; Chen, W.; Xing, F. Pyrolysis Characteristic and Mechanism of Waste Tyre: A Thermogravimetry-Mass Spectrometry Analysis. *J. Anal. Appl. Pyrolysis* **2018**, *129*, 1–5. [CrossRef]
30. Williams, P.T. Pyrolysis of Waste Tyres: A Review. *Waste Manag.* **2013**, *33*, 1714–1728. [CrossRef]
31. Passaponti, M.; Rosi, L.; Savastano, M.; Giurlani, W.; Miller, H.A.; Lavacchi, A.; Filippi, J.; Zangari, G.; Vizza, F.; Innocenti, M. Recycling of Waste Automobile Tires: Transforming Char in Oxygen Reduction Reaction Catalysts for Alkaline Fuel Cells. *J. Power Sources* **2019**, *427*, 85–90. [CrossRef]
32. Seng-eiad, S.; Jitkarnka, S. Untreated and HNO 3 -Treated Pyrolysis Char as Catalysts for Pyrolysis of Waste Tire: In-Depth Analysis of Tire-Derived Products and Char Characterization. *J. Anal. Appl. Pyrolysis* **2016**, *122*, 151–159. [CrossRef]
33. Lin, H.-Y.; Chen, W.-C.; Yuan, C.-S.; Hung, C.-H. Surface Functional Characteristics (C, O, S) of Waste Tire-Derived Carbon Black before and after Steam Activation. *J. Air Waste Manage. Assoc.* **2008**, *58*, 78–84. [CrossRef]
34. López, F.A.; Centeno, T.A.; Rodríguez, O.; Alguacil, F.J. Preparation and Characterization of Activated Carbon from the Char Produced in the Thermolysis of Granulated Scrap Tyres. *J. Air Waste Manage. Assoc.* **2013**, *63*, 534–544. [CrossRef]
35. Wang, M.; Zhang, L.; Li, A.; Irfan, M.; Du, Y.; Di, W. Comparative Pyrolysis Behaviors of Tire Tread and Side Wall from Waste Tire and Characterization of the Resulting Chars. *J. Environ. Manage.* **2019**, *232*, 364–371. [CrossRef] [PubMed]
36. Thommes, M.; Kaneko, K.; Neimark, A.V.; Olivier, J.P.; Rodriguez-Reinoso, F.; Rouquerol, J.; Sing, K.S.W. Physisorption of Gases, with Special Reference to the Evaluation of Surface Area and Pore Size Distribution (IUPAC Technical Report). *Pure Appl. Chem.* **2015**, *87*, 1051–1069. [CrossRef]

37. Sing, K.S.W.; Everett, D.H.; Haul, R.A.W.; Moscou, L.; Pieroti, R.A.; Rouquerol, J.; Siemieniewska, T. Reporting Physisorption Data for Gas/Solid Systems with Special Reference to the Determination of Surface Area and Porosity (Recommendations 1984). *Pure Appl. Chem.* **1985**, *57*, 603–619. [CrossRef]
38. Kyzas, G.Z.; Lazaridis, N.K. Reactive and Basic Dyes Removal by Sorption onto Chitosan Derivatives. *J. Colloid Interface Sci.* **2009**, *331*, 32–39. [CrossRef]
39. Bernardo, M.; Mendes, S.; Lapa, N.; Gonçalves, M.; Mendes, B.; Pinto, F.; Lopes, H.; Fonseca, I. Removal of Lead (Pb2+) from Aqueous Medium by Using Chars from Co-Pyrolysis. *J. Colloid Interface Sci.* **2013**, *409*, 158–165. [CrossRef]
40. Gupta, V.K.; Gupta, B.; Rastogi, A.; Agarwal, S.; Nayak, A. A Comparative Investigation on Adsorption Performances of Mesoporous Activated Carbon Prepared from Waste Rubber Tire and Activated Carbon for a Hazardous Azo Dye—Acid Blue 113. *J. Hazard. Mater.* **2011**, *186*, 891–901. [CrossRef]
41. Karadag, D.; Akgul, E.; Tok, S.; Erturk, F.; Kaya, M.A.; Turan, M. Basic and Reactive Dye Removal Using Natural and Modified Zeolites. *J. Chem. Eng. Data* **2007**, *52*, 2436–2441. [CrossRef]
42. Ozdemir, O.; Armagan, B.; Turan, M.; Çelik, M.S. Comparison of the Adsorption Characteristics of Azo-Reactive Dyes on Mezoporous Minerals. *Dye. Pigment.* **2004**, *62*, 49–60. [CrossRef]
43. Pengthamkeerati, P.; Satapanajaru, T.; Singchan, O. Sorption of Reactive Dye from Aqueous Solution on Biomass Fly Ash. *J. Hazard. Mater.* **2008**, *153*, 1149–1156. [CrossRef]
44. Mui, E.L.K.; Cheung, W.H.; Valix, M.; McKay, G. Dye Adsorption onto Activated Carbons from Tyre Rubber Waste Using Surface Coverage Analysis. *J. Colloid Interface Sci.* **2010**, *347*, 290–300. [CrossRef]
45. Mui, E.L.K.; Cheung, W.H.; Valix, M.; McKay, G. Mesoporous Activated Carbon from Waste Tyre Rubber for Dye Removal from Effluents. *Microporous Mesoporous Mater.* **2010**, *130*, 287–294. [CrossRef]
46. Órfão, J.J.M.; Silva, A.I.M.; Pereira, J.C.V.; Barata, S.A.; Fonseca, I.M.; Faria, P.C.C.; Pereira, M.F.R. Adsorption of a Reactive Dye on Chemically Modified Activated Carbons—Influence of PH. *J. Colloid Interface Sci.* **2006**, *296*, 480–489. [CrossRef] [PubMed]